International Journal of Mass Spectrometry 277 (2008) 284–290

Contents lists available at ScienceDirect

International Journal of Mass Spectrometry

journal homepage: www.elsevier.com/locate/ijms

Structure of neat and hydrated liquid nicotine and laser resonant desorption of clusters from nicotine–water solutions

Claudia Mihesan[a], Michael Ziskind[a], Cristian Focsa[a], Mahamadou Seydou[b], Frédéric Lecomte[b], Jean Pierre Schermann[b,*]

[a] Laboratoire de Physique des Lasers, Atomes et Molécules, UMR 8523 CNRS, Université Lille 1, 59655 Villeneuve d'Ascq cedex, France
[b] Laboratoire de Physique des Lasers, UMR 7538 CNRS, Université Paris 13, 93430 Villetaneuse, France

ARTICLE INFO

Article history:
Received 26 March 2008
Received in revised form 30 June 2008
Accepted 15 July 2008
Available online 20 August 2008

Keywords:
Molecular cluster ions
Nicotine
Infrared spectra
Mass-spectra
Laser resonant desorption

ABSTRACT

The microscopic structures of neat liquid nicotine and nicotine–water mixtures are examined through infrared spectroscopy and laser resonant desorption mass-spectroscopy. The infrared spectra of the solutions are analyzed using DFT calculations of homogenous and mixed hydrogen-bonded clusters. Neat nicotine and hydrated nicotine cluster are experimentally observed through IR laser resonant desorption of a nicotine/water ice mixture followed by laser ionization mass-spectrometry. A sizable fraction of those cluster ions is the result of laser ionization of small neutral clusters already present in the sample.

1. Introduction

Cluster studies offer the possibility to transfer some of the knowledge concerning intrinsic properties of molecules of biological interest acquired from gas-phase experiments to condensed-phase. This has been in particular demonstrated in the case of electron-induced damages to DNA components [1]. An important number of molecules of biological interest concerning humans are produced by other organisms. Among those exogenous molecules, natural substances play an important role as drugs since they can trigger actions similar to those induced by endogenous substances. For example, nicotine is an alkaloid present in several plants and acts as an agonist of the acetylcholine neurotransmitter. Its major source is tobacco leaves and during their humid processing a large amount of nicotine is transferred to water leading to the production of a highly toxic solution [2]. After extraction, nicotine can then be used, for example, in the production of the B3 vitamin (nicotinic acid and nicotinamide) [3]. In the brain, the presence of water molecules influences the binding of nicotine to its receptor (nicotinic acetylcholine receptor, nAChR) [4]. In neat liquid nicotine and in aqueous solution, nicotine molecules are neutral while they become protonated under biological conditions, the pK_A of nicotine being equal to 8.2 as compared to the physiological pH equal to 7.4 [5]. The role of protonation is crucial in the molecular recognition process of nicotine by the acetylcholine receptor. The protonated site of nicotine then plays the role of the positively charged quaternary ammonium of acetylcholine [6].

While neat and hydrated protonated nicotine ions have been the subject of a rather large number of theoretical [6–8] and experimental [9,10] investigations, up to our knowledge, the only structural study concerning the neutral nicotine molecule has been conducted by gas electron diffraction [11]. The present study does not have a direct biological relevance but is rather related to the above presented extraction process of nicotine from plants [2] and its pharmaceutical applications. In the present work, we investigate interactions of nicotine molecules between themselves and with water molecules by means of infrared spectroscopy, quantum chemistry calculations and mass-spectrometry. The structure of neat nicotine and nicotine–water solutions is interpreted in terms of formation of homogeneous and mixed weakly bound clusters. Information concerning those neutral clusters is first obtained through comparison of experimental infrared spectra with simulated spectra derived from electronic structure calculations. The complementary mean of investigation consists in IR laser desorption of frozen water–nicotine solutions. Once neutral clusters are ejected from ice, they are ionized and mass-selected. This provides us the possibility to investigate the existence of neutral clusters issued from the solution through mass-spectrometry. The obser-

* Corresponding author. Fax: +33 1 4940 3200.
E-mail address: jean-pierre.schermann@univ-paris13.fr (J.P. Schermann).

1387-3806/$ – see front matter © 2008 Elsevier B.V. All rights reserved.
doi:10.1016/j.ijms.2008.07.037

vation of parent and daughter cluster ion mass distributions and the analysis of their velocity distributions then provide insights on their origin.

2. Methodology

2.1. Mass-spectrometry of nicotine–water ice

Efficient generation of neat and hydrated nicotine clusters by IR laser resonant desorption of a nicotine/water ice mixture is demonstrated in a two-step laser mass-spectrometry (L2MS) experiment. The samples have been prepared by freezing in liquid nitrogen a 1% solution of nicotine in water (corresponding to a molar concentration nicotine:water 1:900), prior to their insertion in a UHV ($\sim 10^{-9}$ Torr) chamber, onto a temperature regulated sample holder maintained at $T = 90$ K. Laser desorption has been achieved using the output of an optical parametric oscillator (OPO) pumped by a 10 ns pulsed Nd:YAG laser. This OPO was tuned at 3.1 μm in order to excite resonantly the O–H stretching mode of water molecules leading to maximum yield desorption of ice [12]. The maximum energy per pulse used was 2.5 mJ. The laser beam was focused through a CaF_2 lens (100 mm) on the sample surface, leading to fluences ca.1 J/cm^2. The laser–sample interaction leads to vaporization of neutral species (i.e., ions are hardly ever ejected or produced, see Section 3.4.1) from the sample forming a desorption plume propagating normal to the sample surface. The neutral plume is intercepted by the 266 nm beam of a quadrupled Nd:YAG laser used for ionization. Ions were produced directly in the region between the extraction plates of a Wiley–McLaren reflectron time-of-flight mass-spectrometer. Ion detector signals are recorded using a digital oscilloscope (LeCroy) with a time resolution of 0.5 ns.

2.2. Infrared spectroscopy of neat and aqueous solutions of nicotine

The infrared spectra of neat liquid nicotine and a 1:5 nicotine–water solution have been recorded by means of Fourier-transform spectroscopy. 2 μl of each solution were successively deposited on a KBr slide. The IR spectra (Fig. 1) were recorded with a FT-IR Brucker Tensor 27 (2 cm^{-1} resolution). Due to the strong absorption of water above 1700 cm^{-1}, the spectrum of the nicotine–water solution was only recorded in the 800–1600 cm^{-1} fingerprint region.

2.3. Structure calculations

The electronic structures of homogeneous and hydrated neutral and radical nicotine complexes have been determined by optimization of starting structures obtained from a systematic search conducted at the semi-empirical AM1 level. The search degrees of freedom were then the N_{12}–C_{11}–C_5–C_4 torsion angle and the methyl group orientation. The optimizations and analytical frequency calculations were conducted at different levels of theory such as the B3LYP/6-31G* level, the B3PW91/6-311++G** level and the MP2/6-31++G** level according to the number of involved atoms, all using the GAUSSIAN 03 software [13] and a double-core processor (64 bits/2.6 GHz). The optimization procedure was the default termination criteria (Berny algorithm) as implemented in GAUSSIAN 03.

3. Results and discussion

Experimental observation presented here for hydrated nicotine cluster ions can be interpreted in terms of different mechanisms. It is possible to invoke the pre-existence of those clusters in ice and in solution either as charged ions or as neutral species that are further ionized in the gas-phase. It is also possible to invoke aggregation processes taking place during the IR laser resonant desorption/laser ionization. We first investigate the structures of neutral neat and hydrated nicotine clusters and compare their predicted infrared spectra to those experimentally obtained from solutions. We then focus our attention on structures of the hydrated nicotine cluster cations observed through IR laser resonant desorption/laser ionization/mass-spectrometry. The assignment of the mass-spectra, metastable fragmentation and hydrogenation/dehydrogenation processes are then discussed. We then consider the origin of the observed neat and hydrated nicotine clusters.

3.1. Structure of clusters in neutral liquid nicotine

The isolated molecule of nicotine ($C_{10}H_{14}N_2$) possesses an aromatic pyridine cycle linked by the C_5–C_{11} bond to a pyrrolidine cycle (Fig. 2). In its neutral form, the two lowest-energy conformers of the nicotine molecule are labeled Nic(A) and Nic(B) characterized by the N_{12}–C_{11}–C_5–C_4 torsion angle, respectively, equal to 140° and 319°. The relative energy difference $E_A - E_B$ between those two conformers is small and depends upon the level of theory. It is, respectively, equal to +1.78 kJ/mol at the B3LYP/6-31G* level, −2.0 kJ/mol at the B3PW91/6-311++G** level and −2.42 kJ/mol at the MP2/6-31++G** level. The distance between the hydrogen-bond acceptors N_1 and N_{12} of the two cycles is shorter in conformer A than in conformer B (respectively, 4.26 and 4.83 Å). Dimer formation is crucial in neat liquid nicotine since a nicotine molecule can only bind to a single other nicotine molecule. The N_1 atom from the pyridine cycle of a given molecule establishes a hydrogen bond with a C_3–H_8 bond of the pyridine cycle of another molecule (Fig. 2). Due to the presence of its methyl group, the N_{12} atom of the pyrrolidine cycle is much more unfavorable for hydrogen bonding.

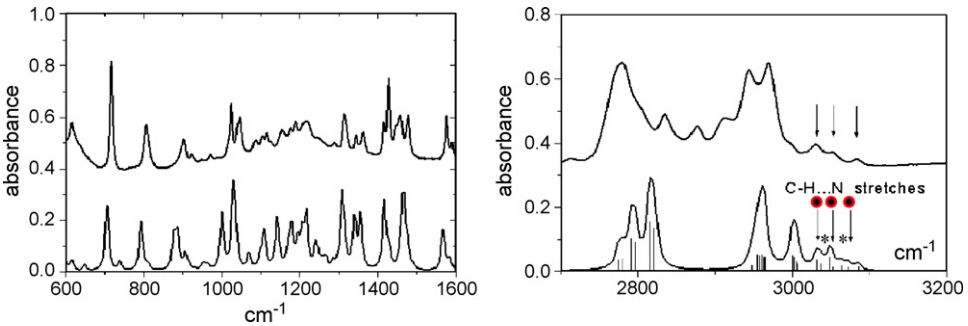

Fig. 1. Experimental (top) and simulated (bottom) infrared spectra of neat liquid nicotine (left) and nicotine in a 1:5 water solution (right). In the right figure, stars correspond to water vibrational modes and circles correspond to concerted vibrational modes involving both nicotine and water molecules.

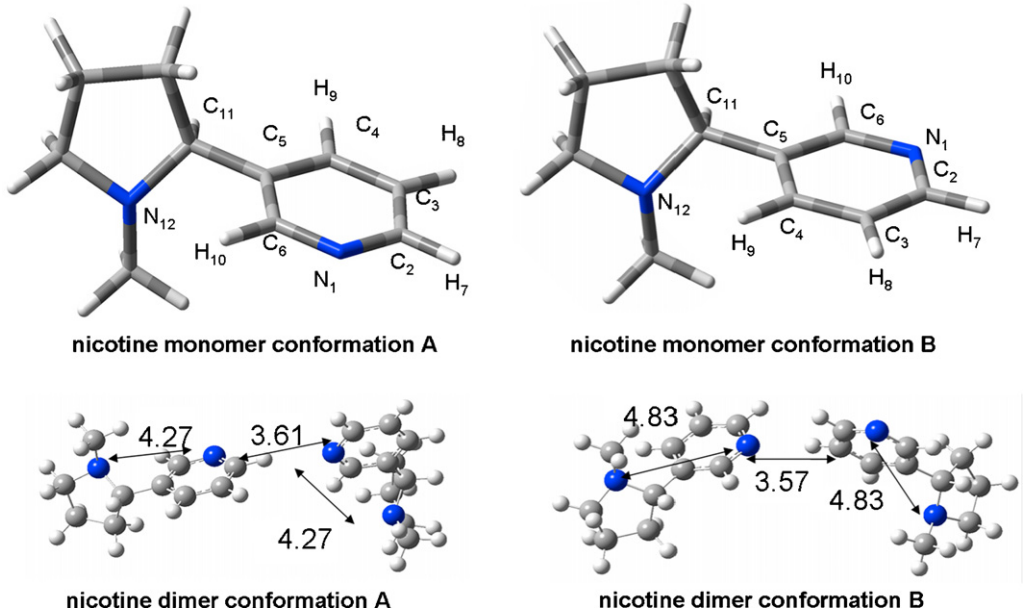

Fig. 2. Top: structures of neutral nicotine conformers A and B. The adopted atom numbering convention is identical to that of Ref. [8]. Bottom: structures of neutral nicotine dimers optimized at the B3LYP/6-31G* level. Intramolecular N_1–N_{12} and intermolecular C_3–$H_8\cdots N_1$ bond distances are in Å.

Intermolecular interactions in liquid nicotine are thus dominated by the C_3–$H_8\cdots N_1$ hydrogen bond and the dispersion interaction between the pyridine cycles.

Binding energies and relative energies of the four possible neutral nicotine dimers have been calculated at the B3LYP/6-31G* level and are provided in Table 1. The most stable homogeneous neutral nicotine dimer is Nic(B)···Nic(B). The mixed Nic(A)···Nic(B) and Nic(B)···Nic(A) dimers are slightly less stable while the Nic(A)···Nic(A) dimer is considerably less stable. The respective strengths of the hydrogen bonding and dispersive interactions have been roughly evaluated by calculating the binding energy of a nicotine molecule to a non-aromatic molecule through an identical C_3–$H_8\cdots N$ hydrogen bond. At this level of theory, hydrogen bonding nearly contributes entirely to the binding energy of the Nic(A)···Nic(A) dimer while it only represents two thirds for the Nic(B)···Nic(B) dimer. However, it must be stressed that DFT calculations strongly underestimate the contribution of dispersion and thus MP2 calculations would be much more preferable.

From the relative energies, we can have a rough estimate of the relative Boltzmann populations in ice solution at 90 K, respectively, equal to 74% (B···B), 14% (B···A), 12% (A···B) and 0.25% (A···A). The situation is rather similar for the respective different binding energies and we can thus conclude that the Nic(A)···Nic(A) dimer does not contribute significantly to the solution structure. The lowest energy structures of the neutral Nic(A)···Nic(A) and Nic(B)···Nic(B) dimers are displayed in Fig. 2.

The optimized neutral nicotine trimer (conformer B) structure calculated at the B3LYP/6-31G* level is provided as Supplementary data. The comparison between the experimental FT-IR spectrum of neat liquid nicotine and the corresponding simulated spectra at the B3LYP/6-31+G* level is displayed in Fig. 2. The IR absorption spectrum of neutral nicotine comprises two well-separated regions. In the 800–1600 cm^{-1} range, the simulated spectra of the neutral monomer and the neutral dimer are both in fair agreement with the experimental spectrum. In this range, the influence of C_3–$H_8\cdots N_1$ hydrogen bond formation is negligible and the infrared absorption properties of liquid neutral nicotine are correctly described by those of the isolated monomer. On the contrary, the absorption spectrum of liquid neutral nicotine in 2500–3200 cm^{-1} range formation is sensitive to the formation of clusters. The spectral signature of C–H···N hydrogen bond formation is provided by the observed red-shifts of the three C–H stretches of the pyridine cycle. Those calculated red-shifts are nearly identical (within 2 cm^{-1}) for the four Nic(A or B)···Nic(A or B) dimers. The values of those red-shifts in the Nic(B)···Nic(B) dimer with respect to the corresponding monomer are given in Table 2. The hydrogen bonds responsible for the formation of clusters in nicotine are very weak as shown by the low values of the induced spectral red-shifts and the large intermolecular C–H···N distances in the 3.5 Å range (Fig. 2).

3.2. Cluster structures in nicotine aqueous solution

In order to interpret the FT-IR spectrum of nicotine in water, neutral nicotine–water complex (further denoted as Nic$(H_2O)_n$) structures have been investigated. The main hydrogen binding sites of neutral nicotine for water molecules are the N_1 and N_{12} atoms, respectively, belonging to the pyridine and pyrrolidine cycle. In the lowest-energy configuration of the Nic$(H_2O)_1$ complex, the water

Table 1
Relative energies and binding energies of the different neutral nicotine dimers calculated at the B3LYP/6-31G* level

Dimer	A···A (kJ/mol)	B···B (kJ/mol)	A···B (kJ/mol)	B···A (kJ/mol)
$E_{relative}$	5.7	0	1.75	1.67
$E_{binding}$	6.6	8.8	8.8	11

Table 2
Experimental and calculated stretch frequencies of the C–H bonds of a pyridine cycle engaged into C–H···N hydrogen bonding with the nitrogen atom of the other pyridine cycle in the neutral Nic(B)···Nic(B) dimer

Vibrational frequency (cm^{-1})	Experimental	Monomer	Dimer
C–H···$N_{sym.}$	3030	3050	3048
C–H···$N_{asym.}$	3052	3070	3063
C–H···$N_{sym.}$	3082	3083	3076

For comparison, the corresponding stretch frequencies are given for the isolated monomer. Those frequencies are calculated at the harmonic B3LYP/6-31+G* level with an applied scale factor equal to 0.9614.

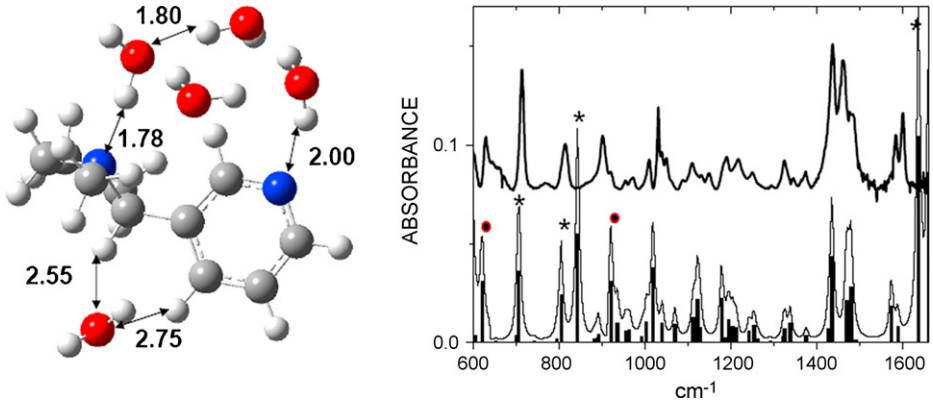

Fig. 3. Left: optimized structure of a Nic$(H_2O)_5$ complex calculated at the B3LYP/6-31G* level (distances are in Å). Right: experimental FT-IR spectrum of nicotine in a 1:5 water solution. Simulated vibrational spectrum (bottom) of the optimized neutral nicotine–[water]$_5$ complex calculated at the B3LYP/6-31G* level. Stars correspond to water vibrational modes and circles correspond to concerted vibrational modes involving both nicotine and water molecules.

molecule establishes a bridge between the two cycles with a strong O–H···N_{12} bond and a weak C_6–H_{10}···O bond. The corresponding binding energy is then rather large as compared to the neat nicotine case and evaluated as 0.41 eV at the B3LYP/6-31G* level (the corresponding structure is provided as Supplementary data). Additional water molecules can bind either to this water molecule then forming a growing water droplet, to the N_1 atom or more weakly through formation of two C–H bonds with binding energies ca. 0.1 eV (Fig. 3). Many local minima coexist on the potential energy hyper-surfaces and a full exploration has not been undertaken. The presented structure is thus only a sample. When the number of water molecules increases, the structure of the nicotine molecule is slightly modified. The N_{12}–C_{11}–C_5–C_4 torsion angle varies from 140° in the monomer to 126° in the mono-hydrated complex and down to 125° in an octo-hydrated complex.

3.3. Structures of neat and hydrated nicotine radical cation clusters

The isolated nicotine radical cation (further denoted Nic^+) has two conformers characterized by the N_{12}–C_{11}–C_5–C_4 torsion angle, respectively, equal to 125° and 300°. The binding energy of the Nic^+···Nic dimer is equal to 0.63 eV at the B3LYP/6-31G* level. Structures of $(Nic^+(H_2O)_n)$ complexes are provided as Supplementary data. In the lowest-energy configuration of the singly hydrated complex, the water molecule dipole is oriented by the positive charge of the nicotine radical cation located on the pyrrolidine cycle. In more hydrated nicotine radical cation complexes, the structure of the water molecule network is the result of the competition between hydrogen bonds and charge–dipole interactions. The N_{12}–C_{11}–C_5–C_4 torsion angle then increases up to 130° in the octo-hydrated complex.

3.4. Neat and hydrated nicotine cluster generation by IR laser resonant desorption

3.4.1. Nicotine: fragmentation, detection efficiency and ionization

A typical result of the IR laser resonant desorption/laser ionization/mass-spectrometry approach applied to a frozen nicotine/water (1%) sample is presented in Fig. 4. The base peak at m/z = 162 corresponds to the intact nicotine radical cation Nic^+. Some fragmentation of nicotine is present as shown in the m/z < 162 region in Fig. 4 but to a less extent than in the case of electron ionization [14–16]. The main fragments are m/z = 39, 42, 55, 65, 84, 93, 105, 119 and 133, corresponding to fragmentation channels already observed in mass-spectrometry studies on nicotine [15,17,18]. Additional signals are detected at m/z = 106 and 147. These products are reported to be formed by nicotine pyrolysis [15,18] in a specific range of temperature (850–950 K). These temperatures are slightly higher than those usually reached by laser resonant desorption of ice in the given experimental conditions (close to the critical temperature of water, T_c = 647 K), leading to a phase-explosion process, i.e., the release of the whole interaction volume into gas phase on a very short time scale [19,20].

In order to evaluate the sensitivity of the method, we below provide an estimation of the desorbed quantity of nicotine per laser shot. The sample volume desorbed by each pulse is approximated as a cylinder of 300 μm length and 0.3 μm diameter. The latter value has been obtained previously for the study of pure ice samples [12,19] and is mainly determined by the optical penetration depth of the laser. In the present case, considering the low concentration of the solution and the lower absorption coefficient of nicotine, as compared to ice at 3.1 μm [21] the optical properties of the samples were approximated by those of pure ice. The desorbed volume is thus 2×10^{-14} m^3 indicating an amount of nicotine as low as ~200 pg available for detection for each laser pulse. This value represents an improvement of several orders of magnitude as compared to the previous results of Morrical and Zenobi [22] who reported a minimum of 10 μg of pure nicotine required to produce a measurable signal by L2MS.

3.4.2. Nicotine clusters: hydrogenation/de-hydrogenation, series assignment, metastable fragmentation

The most important signals detected in the present experiment are due to clusters formed from nicotine in its intact molecular form. Nevertheless, these signals are accompanied by smaller ones with m/z lower or higher by 1 amu than the corresponding clusters, indicating the loss or gain of one hydrogen atom. This kind of hydrogenated and de-hydrogenated clusters are major products of laser desorption/laser ionization of ices doped with oxygen-containing organic molecules (formaldehyde, alcohols) [20,23].

In addition to the intact nicotine cation Nic^+ at m/z = 162, the mass-spectra exhibit a significant amount of de-hydrogenated nicotine (m/z = 161, relative intensity ~20%). This de-hydrogenation process has also been observed in electron impact ionization and most probably occurs in the parent cations. The present degree of de-hydrogenation resulting from laser desorption/laser ionization is however lower than those previously observed by different methods of ionization [14–16,24].

The signal at m/z + 1 is due to the contribution of heavier isotopes (^{13}C, ^{15}N or ^{2}H, ^{17}O) but the addition of H atoms to nicotine molecules or to clusters must also be considered. Indeed, the

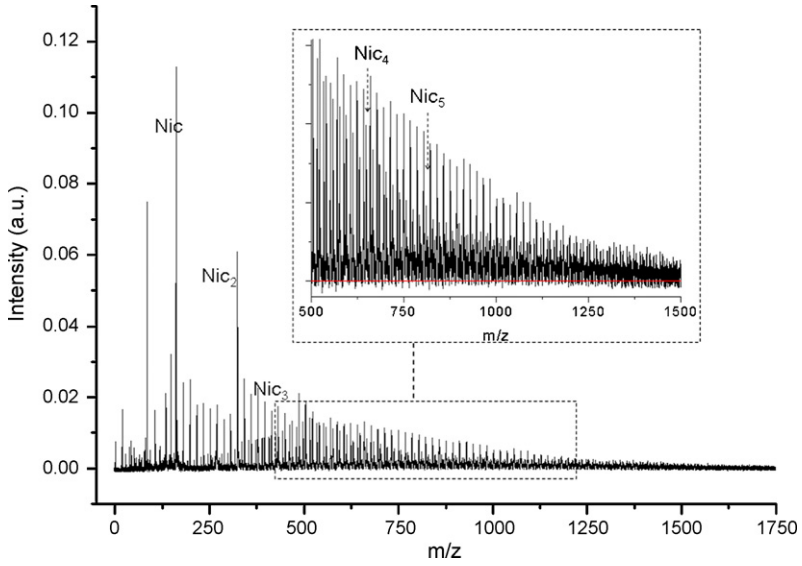

Fig. 4. Overview of the mass-spectrum obtained by IR laser resonant desorption of a nicotine/water ice mixture.

signal intensity is higher than the calculated isotopic contribution (11.8% for nicotine) signifying that the hydrogenated clusters $((Nic)_p(H_2O)_n)H$ are formed in the initial solution or during the desorption/ionization processes. The relative intensity of these signals corrected for the isotopic contribution is ~5–10% of the corresponding $(Nic)_p(H_2O)_n$ hydrated clusters. The predominance of de-hydrogenated over hydrogenated clusters is corroborated by the results of a theoretical study on pyridine ion in water complexes [25] indicating a higher stability for hydrated clusters (1–5 water molecules) formed by one molecular pyridine ion.

The hydrogenation degree (defined as the ratio of hydrogenated over non-hydrogenated species) is more important for the nicotine molecule and for "neat" nicotine clusters as compared to hydrated clusters. Considering the nitrogen atoms (N_1 and N_{12}) as hydrogenation sites, the water molecule(s) in clusters will preferentially occupy these sites (see Fig. 5), hence reducing the hydrogenation probability (see Section 3.2). This is not the case for "neat" nicotine molecules, where only N_1 atom will participate into formation of H-bonds, leaving the N_{12} available for the hydrogenation (see Section 3.1).

De-hydrogenated species are also observed at m/z-1, corresponding to the $(Nic_p(H_2O)_n)$–H series. As the presence of the de-hydrogenated nicotine in the ice sample is very unlikely, the occurrence of these species must be linked to the desorption and/or ionization processes. The same trend observed for hydrogenation of "neat" nicotine vs. hydrated clusters is observed for de-hydrogenation. The lower degree of de-hydrogenation for the hydrated clusters seems to indicate that the availability of H atoms for fragmentation reactions is reduced by the presence of water molecules.

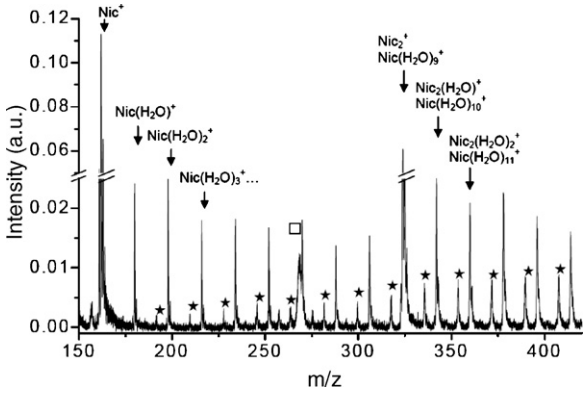

Fig. 5. Zoom on the first $Nic_p(H_2O)_n^+$ clusters. The stars indicate the charged fragments generated by metastable evaporation of one water molecule. The square is associated with metastable dissociation of Nic_2^+ (see text).

The signals detected at $m/z > 163$ correspond to molecular aggregates. Fig. 4 displays an expanded view of a part of the mass-spectrum with the proposed assignment for the most intense peaks. An increment of 18 amu indicates the addition of one water molecule. The $Nic(H_2O)_n$ series can be undoubtedly followed up to $n = 8$. A mass coincidence appears at $m/z = 324$, due to the fact that the mass of nine water molecules equals that of one nicotine molecule. Therefore, this peak can be attributed to both Nic_2 and $Nic(H_2O)_9$ clusters. From here on, each signal at $m/z = p^*162 + n^*18$ can be attributed to $Nic_p(H_2O)_n$, but also to $Nic_{p-1}(H_2O)_{n+9}$, $Nic_{p-2}(H_2O)_{n+18}$, etc. The evolution of the peak intensities in Fig. 5 clearly shows a steep increase above $m/z = 324$ (with respect to the preceding peak evolution). This leads us to consider the contribution of both $Nic(H_2O)_n$ and $Nic_2(H_2O)_{n-9}$ to these signals. Following these assertions and considering Fig. 4, we interpret our experimental spectra as the observation of "neat" Nic_p clusters and associated $Nic_p(H_2O)_n$ hydrated series up to at least $p = 5$ (an estimation of the maximum number n of water molecules in a series will be given further below).

Fig. 5 also displays the presence of another series of peaks (marked with a star), situated at non-integer m/z values. These peaks correspond to "daughter ions" formed by metastable fragmentation of the clusters during the flight through the field-free zone of the mass-spectrometer, due to an excess of internal energy received during the desorption and/or ionization processes. After fragmentation, "daughter ions" possess a velocity equal to that of "parent ions" but have a lower kinetic energy. This reduces the amount of time they spend in the reflectron, making their total time-of-flight shorter than that of the corresponding "parent ions". A theoretical calculation of the time-of-flight for the "parent" and "daughter ions" allowed us to assign the peaks mentioned above to the charged fragments originating from the evaporation of one water molecule: $Nic_p(H_2O)_n^+ \rightarrow Nic_p(H_2O)_{n-1}^+ + H_2O$. The intensity of these fragments with respect to the parent ions increases with the mass, with a maximum in the $m/z = 500$–600 range. Moreover, as the mass increases further more, a second series of daughter

ions appears, with a maximum after $m/z = 1000$. This series is attributed to the fragments generated by the metastable evaporation of two water molecules. At high mass, these daughter ions series will eventually become more intense than the parent series. A more detailed future study of this fragmentation behaviour can offer some hints on the stability of these aggregates. Note also that the "neat" Nic_p clusters can also undergo metastable fragmentation by the loss of one nicotine molecule or other fragments: an example is given in Fig. 5 (peak marked with a square, originating in the dissociation of the dimer ion into a charged and a neutral monomer).

From a practical point of view and in order to evaluate the abundance of the different $Nic_p(H_2O)_n$ clusters produced by desorption/ionization, we also have to consider the contribution of the daughter ions. The evolution with mass of the $Nic_p(H_2O)_n$ signals, the evolution of the fragments generated by metastable evaporation of one and two water molecules, and that corrected for the contribution of the fragments are provided as Supplementary data. A detailed treatment leads to a rough estimation of a maximum number n of water molecules associated with a given $Nic_p(H_2O)_n$ series in the range of 15–20. As measurable signals can still be obtained at m/z as high as 1800, we can then infer a maximum number of nicotine molecules $p \sim 9$. Taking into account this contribution, the increase of signal intensities with addition of even numbers of H_2O molecules, as observable in Fig. 5, is much less marked. This observation might be an information on the relative stability of the cluster in gas-phase rather than in solution.

3.4.3. Origin of the observed neat and hydrated nicotine clusters

A crucial question we now address concerns the origin of the clusters we observe through mass-spectrometry. We wish to examine whether or not those clusters originate from clusters already existing in the solution. Experimentally, we observed that only very few ions are directly ejected from the sample. Those ions do not require the presence of the UV laser and appear in the mass-spectra at negative times since the ionization pulse provides the time origin. Brutschy et al. [26] estimate that about only a fraction of one in 10^4 of solvated ions is ejected. According to the "lucky survivor" model [27], this small efficiency is due to the sudden decrease of water dielectric constant during the very fast non-equilibrium phase transition induced by photon absorption. This facilitates the recombination of the no-longer shielded anions and cations such that only a small fraction of ions can be detected in the experiments. In other words, even if the presence of cations in solution is possible, the desorption process will prevent their direct observation.

In order to get some further insight on the cluster formation mechanism, a study of the evolution of the velocity distribution with the cluster size has been performed by varying the delay Δt between desorption and ionization laser pulses (for details see [20]). The obtained results are similar to those from studies performed on pure water cluster series in Ref. [28]. In particular, we can evidence a clear distinction between heavy and light clusters (roughly, monomers, dimers and with few water molecules). This finding is in agreement with molecular dynamics simulations developed by Zhigilei [29]. Indeed, this theoretical work suggests that the molecules and lightest clusters are ejected from the sample surface with high velocity as a result of the explosive decomposition of the over-heated material, while the heavier clusters should appear as a result of the fast (i.e., during the desorption) evaporation of transient liquid structure and droplets generated by the laser irradiation. Moreover, one can observe in the mass-spectra that the heavier clusters contribution diminishes when they spend more time in the plume. This reveals unambiguously a fragmentation process of these clusters into monomers and smaller size aggregates, taking into account the slow decay of these species in their velocity distributions. This strengthens our hypothesis of the pre-existence of small clusters in frozen solution. However, we must take into account that a fraction of small clusters also results from in-plume processes while the large clusters rather come from the desorption.

4. Conclusion

Neat nicotine and nicotine–water mixtures have been experimentally studied by means of infrared spectroscopy and infrared laser resonant desorption mass-spectrometry. The analysis of infrared absorption spectra of those mixtures has been conducted by means of DFT calculations of the homogenous Nic_n and $Nic(H_2O)_n$ clusters. In neat nicotine, the simulated spectra show that the presence of C–H···N hydrogen bonds is responsible for the formation of homogenous $(Nic)_n$ clusters. Structure calculations also provide the different binding sites of water molecules to neutral and radical cation nicotine in the observed clusters. The major components of the laser resonant desorption mass-spectra of frozen nicotine–water solutions are $(Nic(H_2O)_n)$ and $(Nic_2(H_2O)_n)$ clusters. It is shown that those clusters both originate from the sample and from in-plume fragmentation of larger clusters generated during the desorption process.

Appendix A. Supplementary data

Supplementary data associated with this article can be found, in the online version, at doi:10.1016/j.ijms.2008.07.037.

References

[1] R. Balog, J. Langer, S. Gohlke, M. Stano, H. Abdoul-Carime, E. Illenberger, Int. J. Mass Spectrom. 233 (2004) 267.
[2] A. Shidadeh, R. Saleh, Food Chem. Toxicol. 43 (2005) 655.
[3] R.M. Maduro, M. Aznar, Fluid Phase Equilib. 259 (2007) 83.
[4] S. Amiri, M. Sansom, P. Biggin, Protein Eng. Des. Sel. 20 (2007) 353.
[5] A. Roos, W.F. Boron, Physiol. Rev. 61 (1981) 297.
[6] D.E. Elmore, D.A. Dougherty, J. Org. Chem. 65 (2000) 742.
[7] P.S. Hammond, Y. Wu, R. Harris, T.J. Minehardt, R. Car, J.D. Schmitt, J. Comput. Aided. Mol. Des. 19 (2005) 1.
[8] C. Munoz-Caro, A. Nino, M. Mora, S. Reyes, F.J. Melendez, M.E. Castro, THEOCHEM. J. Mol. Struct. 726 (2005) 115.
[9] J. Graton, M. Berthelot, J.F. Gal, S. Girard, C. Laurence, J. Lebreton, J.Y. Le Questel, P.C. Maria, P. Naus, J. Am. Chem. Soc. 124 (2002) 10552.
[10] M. Seydou, G. Gregoire, J. Liquier, J. Lemaire, F. Lecomte, J.P. Schermann, C. Desfrancois, J. Am. Chem. Soc. 130 (2008) 4187.
[11] T. Takeshima, R. Fukumoto, T. Egawa, S. Konaka, J. Phys. Chem. A 106 (2002) 8734.
[12] C. Focsa, C. Mihesan, M. Ziskind, B. Chazallon, E. Therssen, P. Desgroux, J.L. Destombes, J. Phys. Condens. Matter 18 (2006) S1357.
[13] M. Frisch, J. Trucks, G.W.H.B. Schlegel, G.E. Scuseria, M.A. Robb, J.R. Cheeseman, J.A. Montgomery, T. Vreven, K.N. Kudin, J.C. Burant, J.M. Millam, S.S. Iyengar, J. Tomasi, V. Barone, B. Mennucci, M. Cossi, G. Scalmani, N. Rega, G.A. Petersson, H. Nakatsuji, M. Hada, M. Ehara, K. Toyota, R. Fukuda, J. Hasegawa, M. Ishida, T. Nakajima, Y. Honda, O. Kitao, H. Nakai, M. Klene, X. Li, J.E. Knox, H.P. Hratchian, J.B. Cross, C. Adamo, J. Jaramillo, R. Gomperts, R.E. Stratmann, O. Yazyev, A.J. Austin, R. Cammi, C. Pomelli, J.W. Ochterski, P.Y. Ayala, K. Morokuma, G.A. Voth, P. Salvador, J.J. Dannenberg, V.G. Zakrzewski, S. Dapprich, A.D. Daniels, M.C. Strain, O. Farkas, D.K. Malick, A.D. Rabuck, K. Raghavachari, J.B. Foresman, J.V. Ortiz, Q. Cui, A.G. Baboul, S. Clifford, J. Cioslowski, B.B. Stefanov, G. Liu, A. Liashenko, P. Piskorz, I. Komaromi, R.L. Martin, D.J. Fox, T. Keith, M.A. Al-Laham, C.Y. Peng, A. Nanayakkara, M. Challacombe, P.M.W. Gill, B. Johnson, W. Chen, M.W. Wong, C. Gonzalez, J.A. Pople, Gaussian Package in I. Gaussian (Ed.), Pittsburg, PA, 2003.
[14] F.W. McLafferty, Anal. Chem. 28 (1956) 306.
[15] A.M. Duffield, H. Budzikiewicz, C. Djerassi, J. Am. Chem. Soc. 87 (1965) 2926.
[16] NIST Chemistry WebBook, W.G. Mallard (Ed.), NIST Standard Reference Database.
[17] R.L. Stedman, Chem. Rev. 68 (1968) 153.
[18] J.P. Williams, N.M.M. Nibbering, B.N. Green, V.J. Patel, J.H. Scrivens, J. Mass Spectrom. 41 (2006) 1277.
[19] C. Focsa, B. Chazallon, J.L. Destombes, Surf. Sci. 528 (2003) 189.
[20] C. Mihesan, N. Lebrun, M. Ziskind, B. Chazallon, C. Focsa, J.L. Destombes, Surf. Sci. 566 (2004) 650.

[21] J.M. Garrigues, A. Pérez-Ponce, S. Garrigues, M. de la Guardia, Anal. Chim. Acta 373 (1998) 63.
[22] B.D. Morrical, R. Zenobi, Atmos. Environ. 36 (2002) 801.
[23] M. Ziskind, C. Mihesan, N. Lebrun, B. Chazallon, C. Focsa, J.L. Destombes, Appl. Phys. A 79 (2004) 991.
[24] W.D. Davis, Environ. Sci. Technol. 11 (1977) 593.
[25] M.C. Sicilia, C. Munoz-Caro, A. Nino, Chem. Phys. Chem. 6 (2005) 139.
[26] N. Morgner, T. Kleinschroth, H.D. Barth, B. Ludwig, B. Brutschy, J. Am. Soc. Mass Spectrom. 18 (2007) 1429.
[27] M. Karas, M. Gluckman, J. Schafer, J. Mass Spectrom. 35 (2000) 1.
[28] C. Mihesan, M. Ziskind, B. Chazallon, C. Focsa, J.L. Destombes, Appl. Surf. Sci. 248 (2005) 238.
[29] L. Zhigilei, Appl. Phys. A 76 (2003) 339.